Supplemental Material

Molecular Biology of the Cell

Schaumann, Staddon et al.

Supplemental Movie Legends……1
Computational Model and Methods…….2-5
Figures S1-S9……..6-12

Supplemental Movie Legends

Movie S1: Dynamic traction stresses in a micropatterned colony of motile MDCK cells. (Left) Stargazin-GFP labeled MDCK cells displaying intercalations and movement along with large cell shape changes, while retaining the overall colony shape. (Right) Traction stresses associated with the cells. While traction stresses are present along the colony periphery, they display no preferred orientation with respect to the colony edge.

Movie S2: Movie of a vertex model simulation for a solid-like colony. (Left) Cell shapes and focal adhesion locations for cells on a patterned substrate. (Right) Traction heatmaps associated with the cells shown. Traction stresses are localized almost completely to the colony edge, and maintain a steady-state over the course of the simulation.

Movie S3: Movie of a vertex model simulation for a fluid-like colony. (Left) Cell shapes and focal adhesion locations for cells on a patterned substrate. (Tight) Traction heatmaps associated with the cells shown. Significant traction stresses along the colony interior accompany cell shape changes. Interior traction stresses are also more dynamic in the fluidized case, with appreciable reorganization over the simulation time.

Movie S4: 3.5 hour long movie of the colony featured in Figure 5A. (Left) Phase contrast images showing scarce cell shape change and absence of neighbor exchanges over the duration of the experiment. (Right) Traction heatmaps corresponding to the phase contrast images. Traction stress peaks are predominantly localized to the colony periphery, remain relatively static, and tend to point inward and perpendicular to the colony edge.

Movie S5: 3.5 hour long movie of the colony featured in Figure 5B. (Left) Phase contrast images showing large-scale cell movement, shape changes, and neighbor rearrangements. (Right) Traction heatmaps corresponding to the phase contrast images. Traction stresses are dispersed throughout the colony and hot spots move in conjunction with cellular motions.

Movie S6: Movie of the simulated cell division shown in Figure 6C,D. (Left) Simulation images showing a cell, highlighted in red, undergoing a division. (Right) Traction heatmaps corresponding to the simulation images. Traction is initially localized to the colony periphery. As the dividing cell pinches, traction is localized around the cell and is dissipated once the daughter cells relax.

Movie S7: Movie of the simulated induced cell rotation shown in Figure 7C,D. (Left) Simulation images showing cells in a circular micropattern undergoing spontaneous rotation due to polarity alignment. (Right) Traction heatmaps corresponding to the simulation images. Traction can localize around cells inside away from the colony periphery, and move with the rotating cells.

Computational Model and Methods

Cell-substrate interactions

We model the elastic substrate as a triangular mesh of springs with a spring constant k_s. The Young's modulus is given by $E_s = \frac{2k_s}{\sqrt{3}h_s}$, where h_s is the substrate thickness, and Poisson's ratio $\nu = \frac{1}{3}$. One limitation of this approach is that the Poisson's ratio is fixed at 1/3. Using different networks of springs, such as Delaunay triangulations, triangular meshes with missing edges, or implementing discretized continuum elastic equations on a square mesh allows variations in Poisson's ratios. Using the latter technique, we simulated colonies on substrates with Poisson ratios of 1/2, 1/3 and 1/4. As shown in Figure S7, variations in the Poisson's ratio do not change the traction force patterns for static or motile cells (Figure S7).

Since focal adhesions and cellular traction forces typically localize at the cell periphery, we implement adhesions that connect cell vertices to the substrate mesh. We subdivide cell edges into finer segments to have an even distribution of adhesions around the cell. This has the added effect of allowing cells to take more flexible shapes, with non-straight cell-cell interfaces.

We model the focal adhesion complexes as stiff springs with stiffness k_f, which link the cell vertices with the substrate mesh. Bound focal adhesions can detach stochastically with a rate k_{off} and bind to the substrate with a rate k_{on}. During attachment, the adhesion will attempt to connect the cell vertex to the nearest node of the substrate mesh. If this substrate node is outside of the micropatterned area then adhesions are disallowed. The resultant model can successfully capture traction stress patterns for single cells adherent on micropatterns of different geometries (Figure S8; Oakes, 2014).

Active cell motility

Self-propulsion - Cells within the colony actively move due to self-propulsion forces. Each cell is assigned a unit polarity vector, $\widehat{\boldsymbol{p}}_{\boldsymbol{i}}$, which defines the front and rear polarization of a motile cell. The resultant movement occurs with a velocity equal to $v_0^i \widehat{\boldsymbol{p}}_{\boldsymbol{i}}$ where v_0^i is the internal motility speed of cell i. The polarity of a cell i in the colony interior is defined by a unit vector with angle θ_i that fluctuates due to a Gaussian white noise with mean 0 and variance $2D_r$, resulting in a rotational diffusion rate of D_r. The resultant motility force on vertex α is given by the average force from its neighboring cells:

$$\frac{1}{n_\alpha}\sum_{\alpha \in i} \mu v_0^i \widehat{\boldsymbol{p}}_{\boldsymbol{\imath}}$$

where n_α is the number of cells neighboring vertex α, v_0 is the self-propulsion speed, μ is a friction coefficient, and the sum is over all neighboring cells to vertex α.

Protrusions - Cells at the edge of the colony area can move via protrusive forces. If the polarity vector for a cell at the colony edge points outside of the colony then protrusive forces push cell vertices outwards with force $\boldsymbol{f}_{prot}$ in the direction of movement, before binding to the substrate. Cortical tension in the cell then drags the rear of the cell forward, while the adhesion bonds resist retraction of the protruded edge. This results in a net forward motion of the cell. If the cell moves outside of the adhesive micropattern, protrusions are instead retracted to prevent cell motion outside of the pattern.

Spreading and confinement - Because cells spread over adherent areas and cannot adhere outside of patterned area, cells on the border of the colony can display three distinct types of motion. In the spreading phase, when the cells are fully contained in the pattern the cell polarity points outwards to spread most efficiently. Once the cell reaches the edge of the pattern its polarity vector undergoes Brownian motion with a Gaussian white noise as in the bulk. Once a cell center goes outside of the pattern the cell begins a retreat phase, where its polarity will instead point into the bulk in order to return to the adherent region. These three types of movement ensure that the cells try to maximize spreading on the micropattern without going outside of it.

Alignment of cell motion and polarity

To simulate coordinated rotation in a confined pattern, we introduce alignment interactions between cell polarity vector and velocity. The polarity angle of cell i follows the equation of motion:

$$\frac{d\theta_i}{dt} = \frac{1}{\tau_v}(\theta_i^v - \theta_i) + \xi,$$

where τ_v is the timescale for alignment with the velocity, θ_i^v is the angle of the velocity of the cell center, and ξ is a Gaussian white noise. Cells on the edge of the colony that are more than a cell radius away from the border attempt to move by aligning towards the border, that is

$$\frac{d\theta_i}{dt} = \frac{1}{\tau_v}(\theta_i^v - \theta_i) + \frac{1}{\tau_b}\left(\theta_i^{out} - \theta_i\right) + \xi,$$

where τ_b is the timescale for alignment due to boundary effects, and θ_i^{out} is the angle point towards the border. Similarly, cells that move outside of the pattern will attempt to move back in, that is:

$$\frac{d\theta_i}{dt} = \frac{1}{\tau_v}(\theta_i^v - \theta_i) + \frac{1}{\tau_b}\left(\theta_i^{out} + \pi - \theta_i\right) + \xi.$$

The result of this equation is that cells will align with their neighbors, but the pattern will confine their motion, which can result in coordinated rotation of the colony.

Simulated traction forces and strain energy

At each time step in the simulation we record displacements of the substrate mesh nodes from their initial positions, $\boldsymbol{u} = \boldsymbol{r} - \boldsymbol{r}_0$. We then interpolate the displacement onto a square grid to give us a displacement field. The strain tensor is evaluated using the finite difference discretization of $\epsilon_{kl} = \frac{1}{2}(\partial_k u_l + \partial_l u_k)$, where k and l are in-plane special coordinates. The stress tensor is given by:

$$\sigma_{kl} = \frac{E_s h_s}{(1+\nu)(1-2\nu)}\delta_{kl}\epsilon_{mm} + \frac{E_s h_s}{(1+\nu)}\epsilon_{kl},$$

where h_s is the substrate thickness. The traction stress is calculated using $T_k = \partial_l \sigma_{kl}$, and the strain energy density is given by $U = \frac{1}{2}\epsilon_{kl}\sigma_{kl}$.

To measure strain energy density as a function of distance, we calculate the mean strain energy within distance bands of width dx, so the n^{th} plot in Figures 2C and 3B is the mean strain energy within a distance $[n\,dx, (n+1)dx]$ of the colony border. The strain energy localization parameter

used in Figure 3D is defined as the total strain energy within 10 μm of the colony border (approximately one cells radius), divided by the total strain energy in the substrate.

Cell division

To simulate a dividing cell (Figure 6), we implemented the mechanics of cell division in four steps. First the cell doubles in size, by doubling its preferred area and multiplying its preferred perimeter by $\sqrt{2}$, followed by mechanical relaxation. In the rounding phase, an additional line tension is added to the cell edges, increasing linearly from 0 to Λ_{div} over 6 minutes. Next, a new edge is created between vertices on opposite sides of the cell, chosen to bisect the cell. This new mid-cell edge mimics the actomyosin contractile ring that generates the cleavage furrow of a mitotic cell. Tension builds up on the mid-cell edge, 0 to Λ_{div}, (and is removed on the cell exterior) over 6 minutes as the cell constricts into two parts. Once the mid-cell edge shrinks to zero length, the cell is divided into two daughter cells. The tension at the daughter cell-cell interface is reduced over 9 minutes and the system is allowed to relax (See Figure S4).

Model implementation

AAVM is implemented using Surface Evolver (Brakke, 1992). For a given a micropattern geometry, we generate cells using a Voronoi tessellation of the pattern. Cells are first relaxed to their mechanical equilibrium state, to ensure that they are at an energy minimum, and then adhesive interactions are turned on. We then simulate the colony dynamics by executing the following steps at each time step (Figure S9):

- Update polarity vectors. Cells in the bulk experience rotational diffusion of their polarity. Cells on the border either crawl outwards if there is space, experience rotational diffusion if they are near the micropattern border, or attempt to move back into the colony if they are outside of the pattern.
- Update adhesion states for cell vertices. Vertices with adhesions attempt to unbind at rate k_{off} and vertices without adhesions bind with rate k_{on}.
- Move the cell and substrate vertices by applying mechanical and active forces according to their equations of motion.
- Refine cell edges. Subdivide cell edges over length L_{max} by splitting the edge into two new edges. This allows cell-cell interface to take more flexible shape. Merge cell edges under length L_{min}, by removing the middle vertex. This keeps the density of adhesions around the cell constant.
- Perform neighbor exchanges, also known as T1 transitions, when a cell edge length is shorter than the threshold length, L_{T1}, only if the move lowers the total mechanical energy of the cells.

Each simulation is run for 5 hours, or 10000 time steps. Statistics, such as mean strain energy, traction stress decay length, intercalation rates, and traction stress maps are all averaged over time. Strain energy density as a function of distance is calculated from data at each time point.

Simulation parameters

The table below lists the default simulations parameters, which are used unless explicitly stated, such as using different micropattern curvatures in Figure 3. Where possible, approximate parameter values were taken from experiments, such as cell area, cell count, micropattern size and shape, substrate stiffness. The preferred shape index was chosen to be close to that of

regular hexagons, below the critical value, allowing us to study the effects of cell shape on fluidity near the solid-fluid boundary value.

Surface Evolver uses dimensionless units, so we non-dimensionalize lengths by the length scale of a typical cell, L^*, forces by a force scale $F^* = KL^{*3}$, and time by time scale T^* when implementing the model.

Next, we fit the cell area elasticity, contractility, protrusive forces and focal adhesion parameters to the traction forces generated by the static cells colonies. We compare the traction force magnitudes and spatiotemporal dynamics: in experiments traction forces localized to the colony periphery but would fluctuate in magnitude over time. Lower the adhesion unbinding rate would give a more uniform traction stress around the boundary, while a higher unbinding rate would give more localized patches of traction force on the periphery. An additional contractile tension, γ_{ext}, is added to cell edges at the colony boundary to account for the absence of cell-cell adhesions. Finally, the simulation time scale, cell internal motility speeds, and rotational diffusion of cell polarity were fit to match cell trajectories, and cell crawl speeds in the static case.

Table S1: Default parameter values in AAVM

Parameter	**Default value**
Cell	
Area elastic modulus, K	$0.0666\ \mathrm{nN\ \mu m^{-3}}$
Preferred area, A_0	$225\ \mu\mathrm{m}^2$
Contractile tension, Γ	$15\ \mathrm{nN\ \mu m^{-1}}$
Preferred shape index, $p_0 = P_0/\sqrt{A_0}$	3.6
Additional division tension, Λ_{div}	$66.6\ \mathrm{nN}$
Protrusion force, f_{prot}	$1125\ \mathrm{nN}$
External line tension, γ_{ext}	$112.5\ \mathrm{nN}$
Internal motility speed, v_0	$30\ \mu\mathrm{m\ hr^{-1}}$
Rotational diffusion, D_r	$10\ \mathrm{hr^{-1}}$
Substrate and adhesion	
Young's modulus, E_s	$4\ \mathrm{kPa}$
Poisson's ratio, ν	$1/3$
Thickness, h_s	$7.5\ \mu\mathrm{m}$
Adhesion stiffness, k_f	$60\ \mathrm{nN\ \mu m^{-1}}$
Adhesion binding rate, k_{on}	$500\ \mathrm{hr^{-1}}$

Bulk adhesion unbinding rate, k_{off}	$50\ \mathrm{hr}^{-1}$
Other	
Friction, μ	$2.7\times10^{3}\ \mathrm{nN\ \mu m^{-1}s}$
Simulation time step	$1.8\ \mathrm{s}$
Micropattern area	$6750\ \mu\mathrm{m}^2$
Micropattern curvature	$36.75\ \mu\mathrm{m}$
Cell count	30
T1 threshold length	$1.5\ \mu\mathrm{m}$
Minimum cell edge length	$1.5\ \mu\mathrm{m}$
Maximum cell edge length	$7.5\ \mu\mathrm{m}$
Simulation length scale, L^*	$15\ \mu\mathrm{m}$
Simulation time scale, T^*	$180\ \mathrm{s}$
Simulation force scale, F^*	$225\ \mathrm{nN}$

Comparisons between cell-based and continuum models

The continuum and the active vertex models for the epithelial colony share some common features including tension and elasticity in the colony, coupling of cells to adhesions and the substrate, and explicit control of substrate elasticity and geometry. The key differences are:

- Continuum model of the cell colony assumes fixed materials property of the tissue, specifically an isotropic and homogeneous contractile media governed by linear elasticity. By contrast, tissue mechanical properties in the vertex model are heterogeneous, dynamic, and can exhibit nonlinear response. Furthermore, solid-fluid behavior of the tissue can be tuned locally in the vertex model, which is not possible in a continuum model.
- Continuum model of the colony cannot model active cell-level behaviors such as motility, division, and intercalations that can be naturally implemented in the vertex model.
- Cell-cell interactions (such as adhesive interactions) can be dynamically and spatially controlled in the vertex model. This is not possible in the continuum model.
- In the vertex model, coupling with the substrate can be spatiotemporally controlled. Local cell movement and cell-matrix adhesion binding/unbinding can generate interior traction stresses. Such behaviors are beyond the scope of our continuum model.

References

Brakke, K.A., (1992). The surface evolver. Experimental Mathematics *1*, 141-165.

Oakes, P.W., Banerjee, S., Marchetti, M.C., and Gardel, M.L. (2014). Geometry regulates traction stresses in adherent cells. Biophysical journal *107*, 825-833.

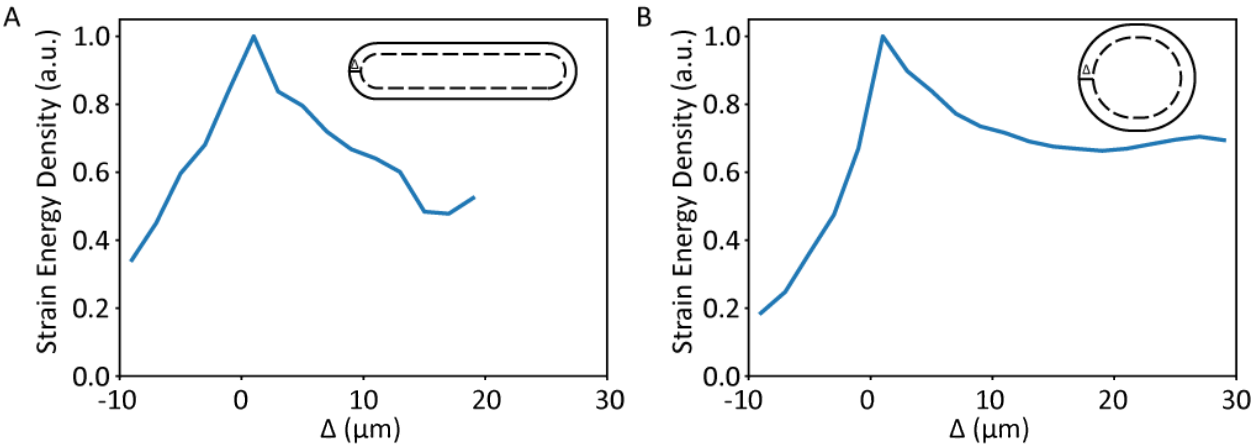

Figure S1: Strain energy profiles for simulated colonies with equal areas and varying radii of curvature. Colonies of both geometries exert stresses primarily at the colony periphery, at the elongated special case, (A) r = 22 μm, as well as the nearly circular case, (B) r = 46 μm.

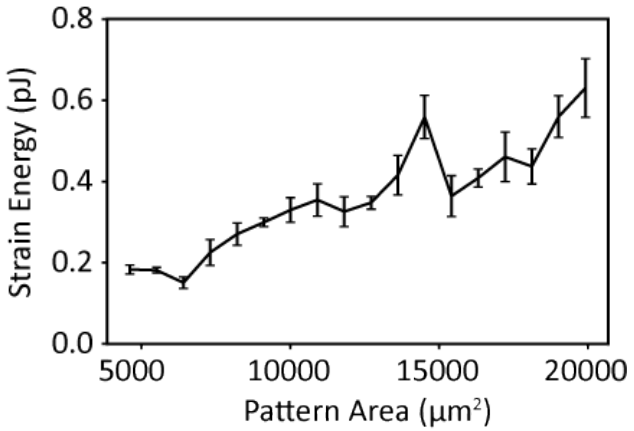

Figure S2: The vertex model predicts that the strain energy produced by a colony scales linearly with colony area. This is in agreement with published experimental results for colonies (Mertz et al., 2012; Mertz et al., 2013) and single cells (Oakes et al., 2014).

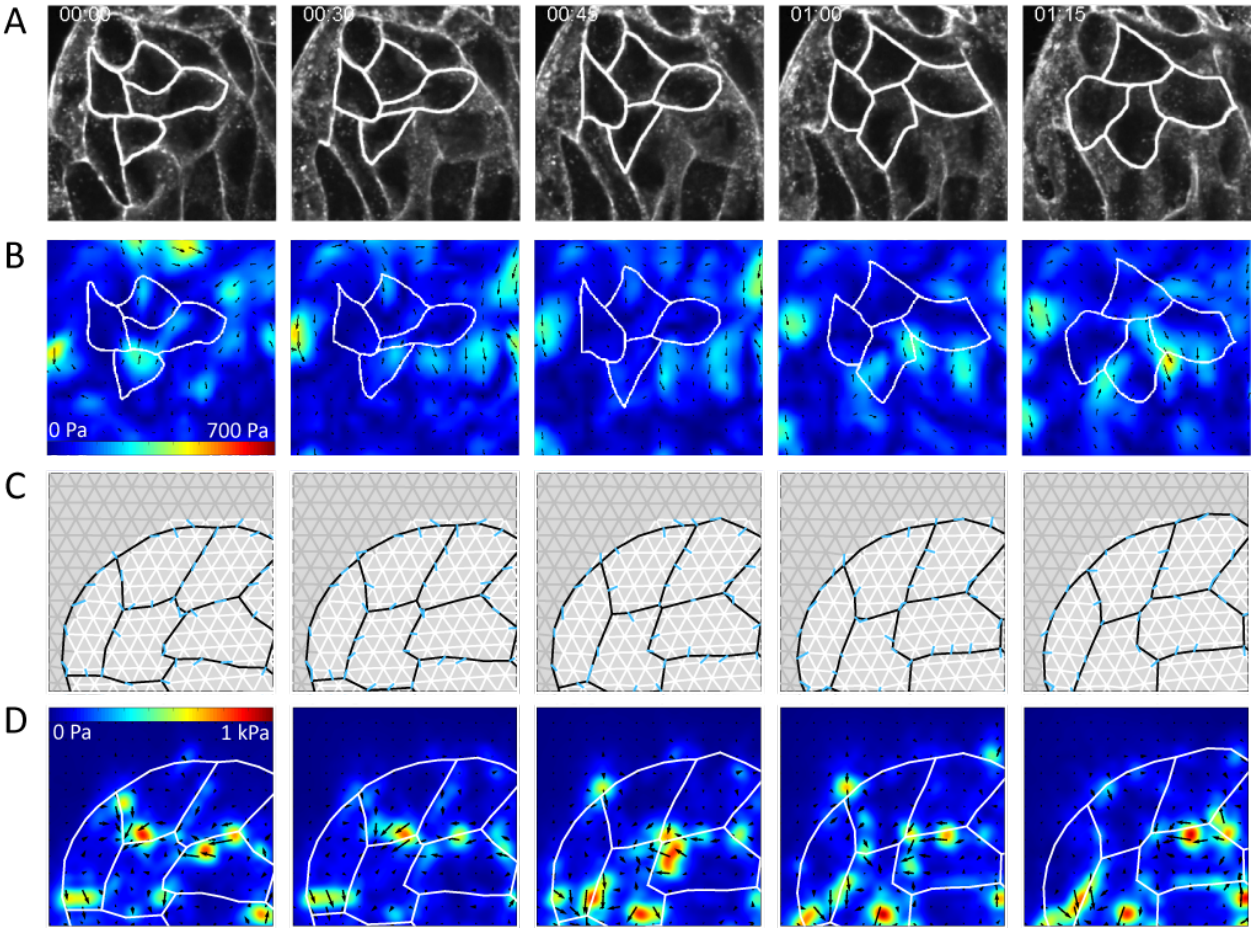

Figure S3: Traction stresses associated with cell neighbor exchanges. (A) Stargazin-GFP images of a portion of the colony from Movie S1 over the course of a neighbor exchange. The four participant cells are outlined in white. (B) Traction maps corresponding to (A), showing traction stresses in the vicinity of the exchange event. (C) Cell shapes during a simulated neighbor exchange for a comparable colony. (D) Traction maps corresponding to the event simulated in (C).

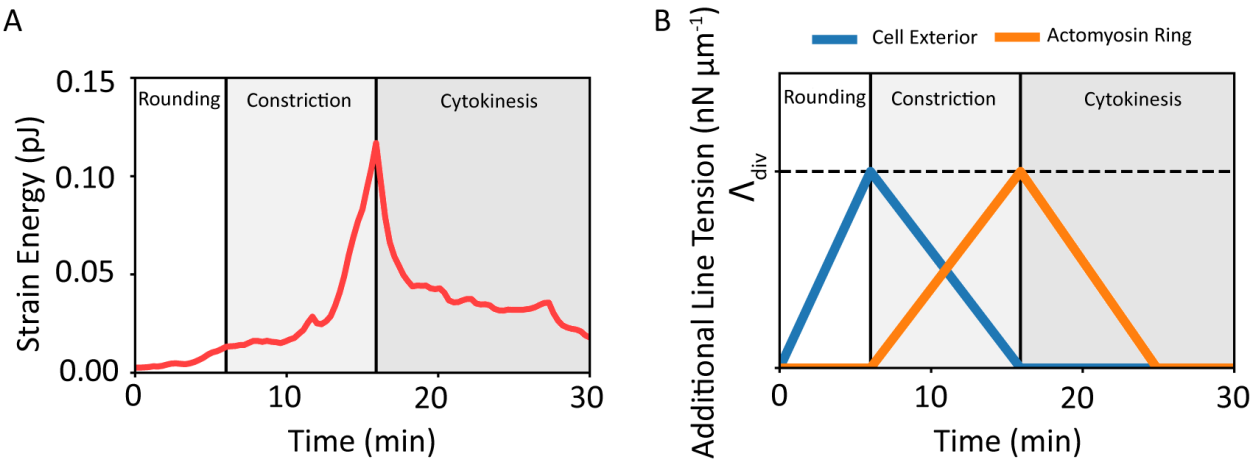

Figure S4: (A) Strain energy increases during the simulated cell division process, and dissipates after the division is over. The initial rounding phase produces only a modest elevation in stresses, but increased tension along the periphery of the mitotic cell leads to a dramatic increase in strain energy. After the splitting phase, the daughter cells relax their tension and the strain energy is concomitantly reduced. (B) Additional line tensions during the different phases of cell division. The actomyosin ring is an edge that connects vertices on opposite sides of the side. As its tension increases the cell pinches in two. After the cell divides, this edge becomes the interface between the two daughter cells.

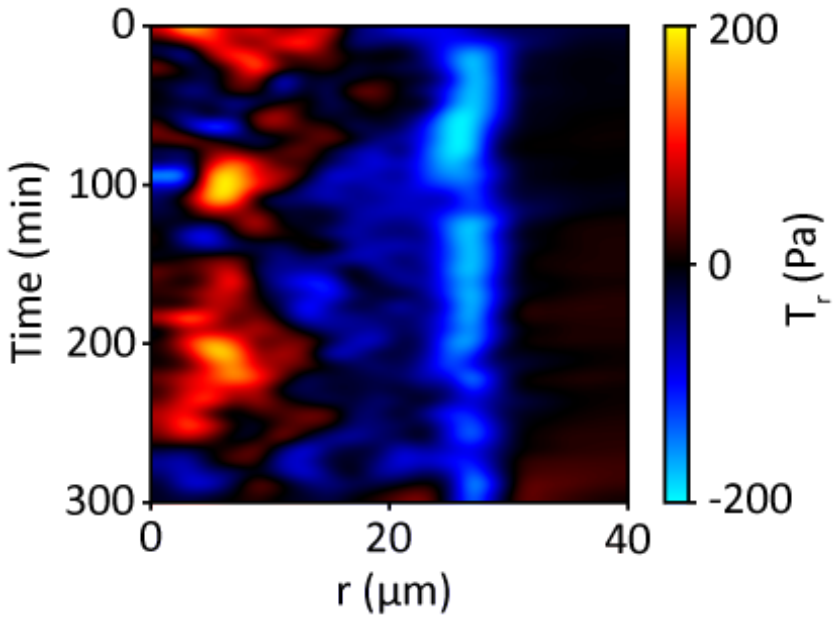

Figure S5: Kymograph for radial traction stress during a simulated collective cell rotation. Traction stresses were averaged over all azimuthal angles to obtain a radial profile of stresses over time. While the most peripheral significant stresses are uniformly pointed inward, stresses in the colony interior fluctuate, with a preference shown towards outward orientation.

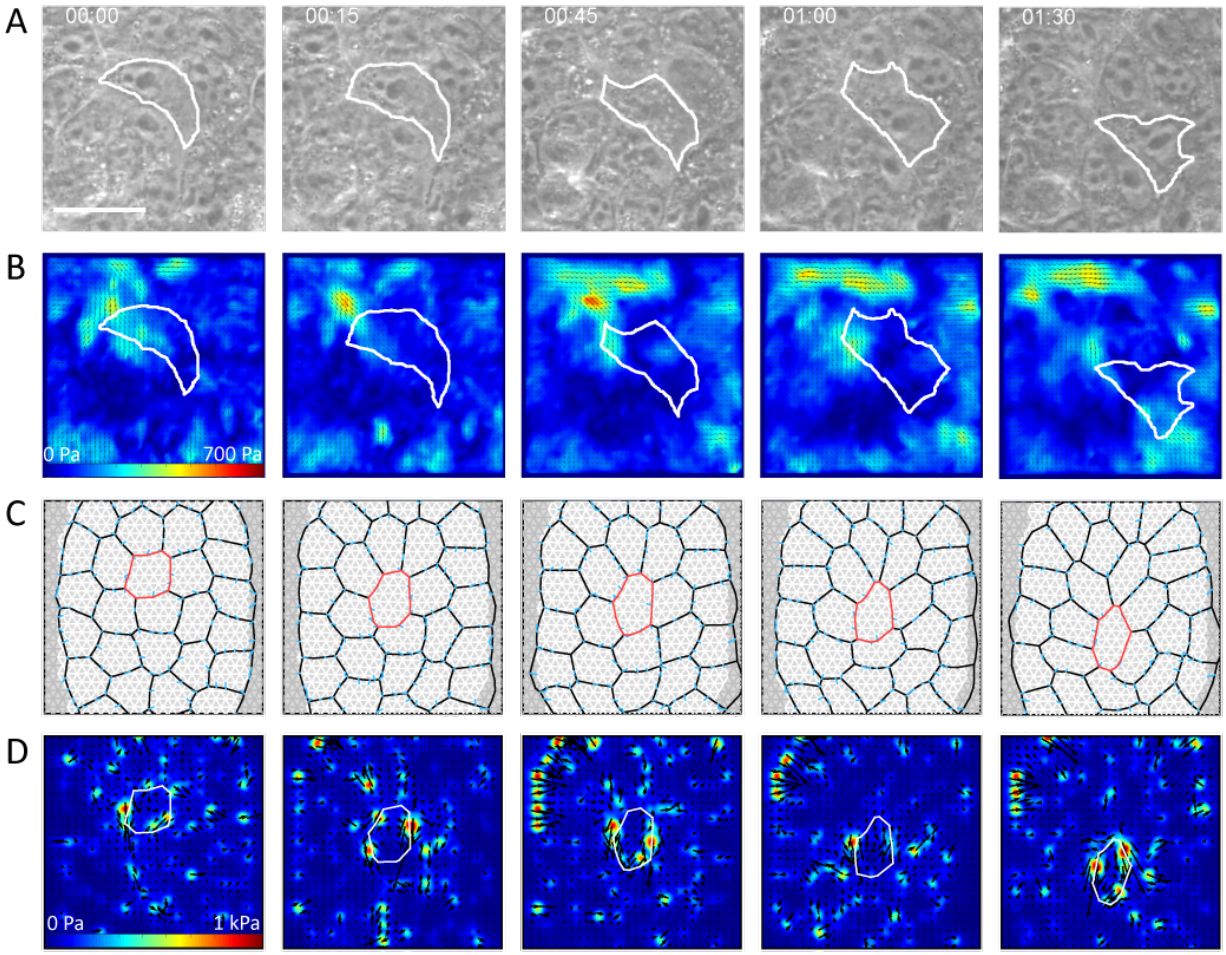

Figure S6: Traction stresses associated with high single-cell motility within a colony. (A) Phase contrast images of a cell moving through the bulk of a colony of MDCK cells. The motile cell is outlined in white. (B) Traction stress heatmaps corresponding to the images in (A), showing a small peak in the stresses that appears to follow one of the cell vertices along the trailing edge, although the specific location is limited by the size resolution of stress peaks. (C) Vertex model simulation of a cell deforming and moving through the colony bulk. The motile cell is outlined in red. (D) Traction stress heatmaps corresponding to the simulated cell shapes in (D), demonstrating the accumulation of stresses along vertices on both the leading and trailing edges of the motile cell.

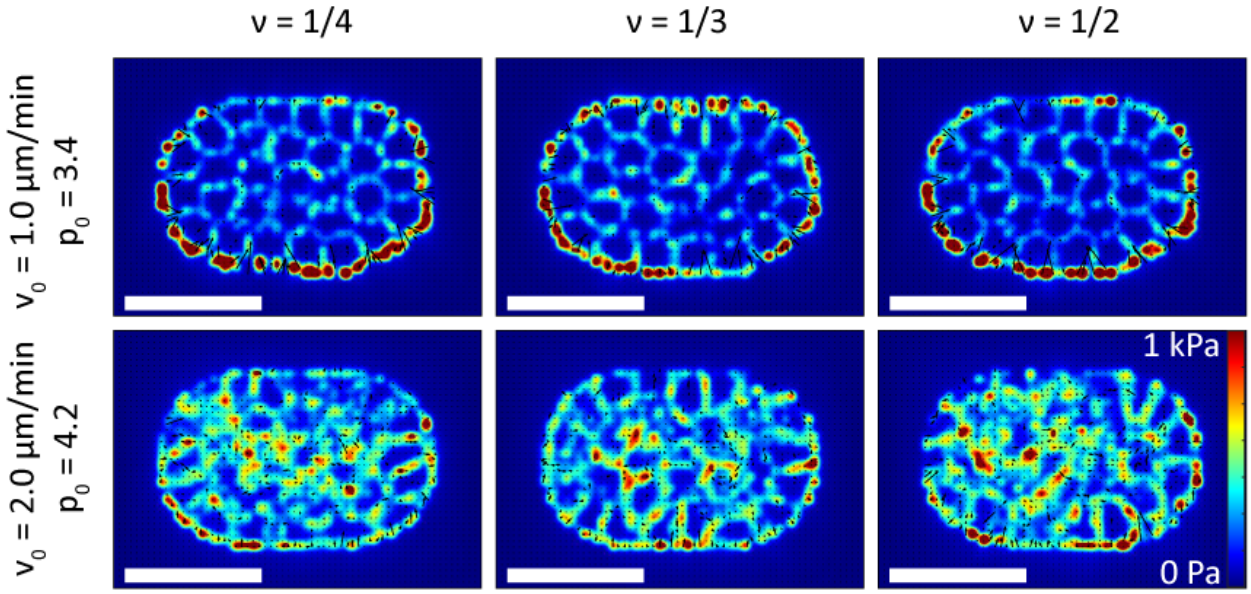

Figure S7: Time averaged traction stress maps for static and motile cell colonies on substrates with varying Poisson's ratio. Using equations of linear elasticity and a square substrate grid, arbitrary Poisson's ratio may be used. Regardless of the Poisson's ratio, traction stresses localize around the colony periphery for low motility (top) and internalize at high motility (bottom). Scale bar represents 50 μm.

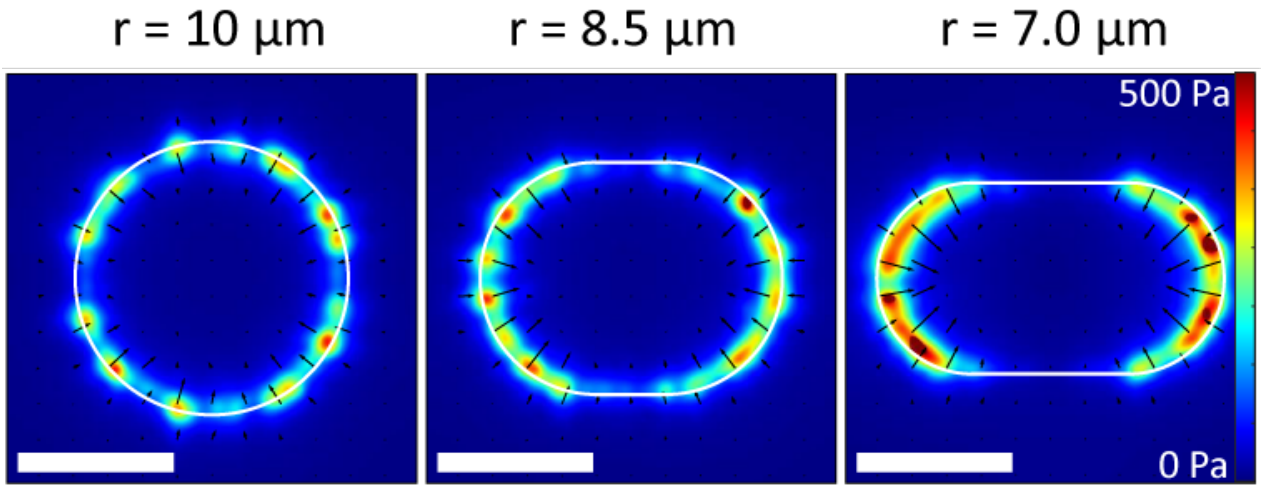

Figure S8: Time averaged traction stress maps for single cells in micropatterns with varying curvature. Traction stresses are localized around the curved borders, and increase in magnitude as the curvature increases. Scale bar represents 10 μm.

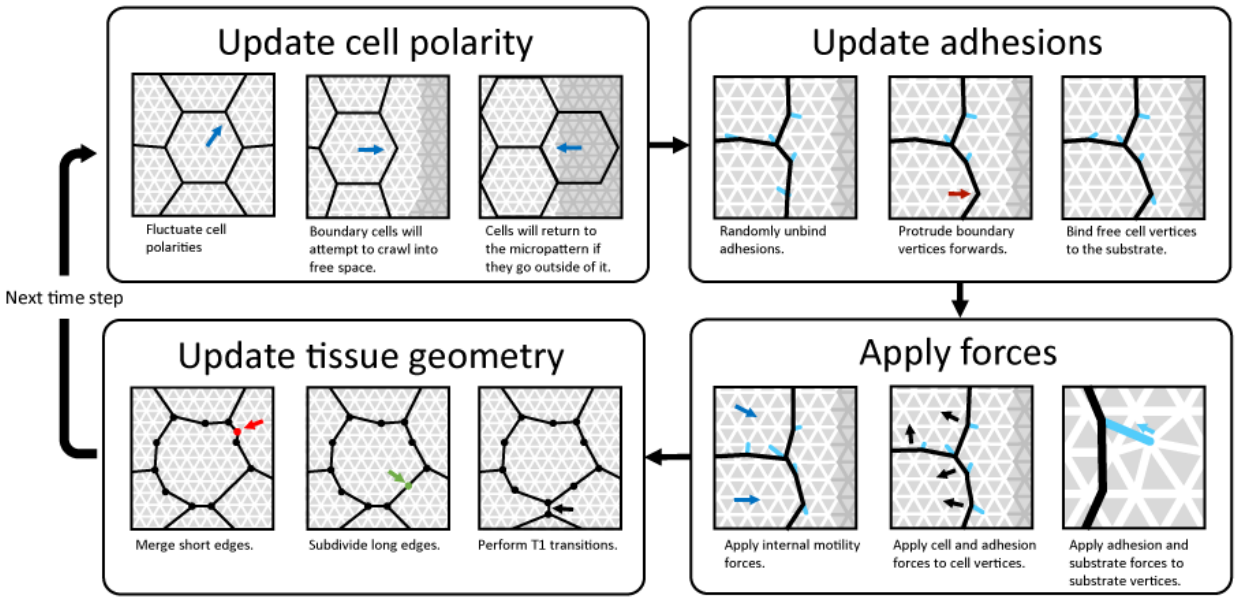

Figure S9: Schematic illustrating the computational pipeline in AAVM.